EUROPEAN ORGANIZATION FOR NUCLEAR RESEARCH

THE INFLUENCE OF ELECTROMAGNETIC INTERACTION ON PROTON-PROTON ELASTIC SCATTERING

J. Bystricky*), A. Gersten**), A. Junod***) and F. Lehar*)

CERN, Geneva, Switzerland

ABSTRACT

Different ways of treating the electromagnetic interaction in proton-proton scattering for energies between 20-750 MeV have been tested using phase-shift analysis. New formulae are presented in order to obtain a good separation of the nuclear and electromagnetic phase shifts. Inclusion of the electromagnetic form factors improves the analysis above 300 MeV, but from the analysis it was not possible to come to conclusions on the shape of the form factors. The $pp\pi^0$ pseudo-vector coupling constant used in the phase-shift analysis was varied and the χ^2 surface was studied in six energy intervals.

Geneva - 26 July 1976

(Submitted to Nuclear Physics B)

---

*) D.Ph.P.E., CEN-Saclay, France.

**) University of Geneva, Switzerland.

***) ETH, Zurich, Switzerland.

1. INTRODUCTION

An accurate treatment of the electromagnetic (e.m.) interaction between two protons is necessary in order to perform a precise analysis of proton-proton (pp) scattering data. We were interested in this problem for two reasons: firstly, to separate properly the e.m. and nuclear interactions in a phase-shift analysis in order to treat pp and np data together; secondly, we are interested in the possibility of obtaining some information about the nuclear amplitudes directly from measurements at small angles [1] in the interference region.

In recent pp phase-shift analyses [2,3] below 1 GeV the statistical errors for some of the partial waves are comparable with some theoretical uncertainties in the determination of the e.m. phase shifts. It was shown by Breit and Ruppel [4] that magnetic moment corrections are important in the description of the small angle pp polarization. But the lowest-order correction introduced by them was insufficient to remove a small discrepancy between their phase-shift predictions and the experimental data. Finally, they were able to remove this discrepancy by dividing the phase shifts into two groups, one for high angular momentum (L) and the other for low L. They have stated that the wave-function distortion is largest in the low L group and that it is not necessary to calculate its effects because the phase shifts can be determined by the search procedure. Although the fit to the experimental data has become better, there still remains one deficiency in this treatment, namely that for the low L group the phase shifts obtained are not well separated from the e.m. phase shifts. The aim of our work is to overcome this deficiency. For this purpose, the following steps have been taken:

i) We have calculated the e.m. phase shifts on the basis of recent interpretations of the sum of divergent partial waves of the e.m. interactions by means of distributions [5,6]. Because the e.m. coupling constant is small, it was possible to perform a systematic evaluation of the e.m. phase shifts in terms of Feynman diagrams.

ii) We have included in our analysis the e.m. form factors of the proton. It seems that by including them there is no need for the separation into the two groups, low and high L partial waves, for which the e.m. contributions should be treated differently.

The method of our phase-shift analysis (Section 2) is based on an earlier work of Bystricky and Lehar [3]. In this analysis we still maintain the low and high L separation of the one-pion exchange (OPE) contribution. By means of χ^2 analysis we have studied the sensitivity of the fit to the experimental data to the change of the pion-nucleon coupling constant of the higher L waves. The

Below we list the helicity amplitudes of the one-photon exchange pp interaction and their partial wave expansions. The results are derived using the techniques and formulae of Gersten et al. [10] and Eq. (1):

$$\phi_1(\theta) = -p^{-1}\left\{f_1/\left[(1-\cos\theta) - f_{10} + 3f_{11}\cos\theta\right]\right\} = \frac{1}{p}\sum_{J=0}^{\infty}(2J+1)\,\phi_1^J\,P_J(\cos\theta)\,, \quad (3)$$

$$\phi_2(\theta) = p^{-1}\left[f_{20} + 3f_{21}\cos\theta\right] = \frac{1}{p}\sum_{J=0}^{\infty}(2J+1)\,\phi_2^J\,P_J(\cos\theta)\,, \quad (4)$$

$$\phi_3(\theta) = \frac{1}{2}\,p^{-1}(1+\cos\theta)\left\{-f_3/\left[(1-\cos\theta) + 3f_{31}\right]\right\} = \frac{1}{p}\sum_{J=1}^{\infty}(2J+1)\,\phi_3^J\,d_{11}^J(\theta)\,, \quad (5)$$

$$\begin{aligned}\phi_4(\theta) = -\phi_2 &= \frac{1}{2}\,p^{-1}(1-\cos\theta)\left\{-2f_4/\left[(1-\cos\theta) + 3f_{41}\right]\right\} = \\ &= \frac{1}{p}\sum_{J=1}^{\infty}(2J+1)\,\phi_4^J\,d_{-11}^J(\theta)\,,\end{aligned} \quad (6)$$

$$\phi_5(\theta) = p^{-1}\left\{f_5/\left[(1-\cos\theta) - \frac{3}{\sqrt{2}}f_{51}\right]\right\}\sin\theta = \frac{1}{p}\sum_{J=1}^{\infty}(2J+1)\,\phi_5^J\,d_{10}^J(\theta)\,, \quad (7)$$

where

$f_1 = \eta(M^2 + 2p^2)/(ME) = \eta_R$

η = $e^2M/(2p)$ is the Coulomb parameter ($e^2 = 1/137.036$)

M is the proton mass

p is the c.m. momentum

$E = (p^2 + M^2)^{\frac{1}{2}}$

$f_{10} = \eta\left[(M/2E) - (2\nu p^2/ME) - (\nu^2p^2/4ME)\right]$

$f_{11} = \eta\nu^2p^2/12ME$

ν is the anomalous magnetic moment of the proton = 1.792846

$f_{20} = \eta\left[(M/2E) - (\nu p^2/ME) + (p^2\nu^2/4ME) + (p^4\nu^2/2M^3E)\right]$

$f_{21} = \eta p^2\nu^2/12ME$

$f_3 = \eta_R = f_1$

$f_{31} = \eta\nu^2p^2/6ME$

$f_4 = \eta\left[(M/2E) - (\nu p^2/ME) + (p^4\nu^2/2M^3E) + (p^2\nu^2/2ME)\right]$

$f_{41} = \eta\nu^2p^2/6ME$

Fortunately enough the resulting divergent series (which have a meaning in terms of distributions) can be summed analytically for most of the terms. All singular terms (which contribute mostly in the forward direction) are obtained in an analytic form. We obtain the following result (the details of the calculations are given in a separate paper [6]):

$$\Delta = \frac{1}{2}\,(1 - \cos\theta)$$

$$p\ \mathrm{Im}\,\phi_1(\theta) = f_1^2\,\frac{\ln\Delta}{2\Delta} - 2f_5^2\,\ln\Delta + g_{10} + 3g_{11}\cos\theta \tag{11}$$

$$p\ \mathrm{Im}\,\phi_2(\theta) = -2f_5^2\,\ln\Delta + g_{20} + 3g_{21}\cos\theta \tag{12}$$

$$\begin{aligned} p\ \mathrm{Im}\,\phi_3(\theta) = {} & \frac{1}{2}\,\eta_R^2(1+\cos\theta)\,\frac{\ln\Delta}{2\Delta} + 3g_{31}\,d_{11}^1(\theta) + \\ & + \frac{1}{2}\,(1+\cos\theta)(\eta_R^2 - 2f_5^2)\,\ln\Delta + \left(f_4^2 - \frac{3}{4}\,\eta_R^2\right)\sum_{J=1}^{\infty}(2J+1)\,\frac{d_{11}^J(\theta)}{J^2(J+1)^2} + \\ & + (2f_5^2 - \eta_R^2)\sum_{J=1}^{\infty}(2J+1)\,x_J\,d_{11}^J(\theta) \end{aligned} \tag{13}$$

$$p\ \mathrm{Im}\,\phi_4(\theta) = \frac{1}{2}\,f_4\eta_R\,\ln\Delta + 2f_5^2 + 3g_{41}d_{-11}^1(\theta) + \frac{1}{2}\,f_4\eta_R\sum_{J=1}^{\infty}\frac{(2J+1)d_{-11}^J(\theta)}{J^2(J+1)^2} \tag{14}$$

$$\begin{aligned} p\ \mathrm{Im}\,\phi_5(\theta) = {} & \frac{1}{2}\sin\theta\left[\eta_R f_5\,\frac{\ln\Delta}{\Delta} - f_5\left(\frac{3}{2}\,\eta_R - f_4\right)\left(\frac{1}{\sin(\theta/2)} - \ln\frac{1+\sin(\theta/2)}{\sin(\theta/2)}\right)\right] + \\ & + f_5\sum_{J=1}^{\infty}\left[J(J+1)\right]^{-\frac{1}{2}}\left[\left(\frac{3}{2}\,\eta_R - f_4\right)\Big/(J+2)\right] + \left[\eta_R/J\right]\ d_{10}^5(\theta) + \\ & + 3g_{51}\,d_{10}^1(\theta)\ , \end{aligned} \tag{15}$$

where

$$g_{10} = f_{10}^2 + f_{20}^2$$

$$g_{11} = f_{11}^2 - 2\eta_R U_1 f_{11} + f_{21}^2 + 2f_{51}^2 + \sqrt{8}\ f_5 f_{51}$$

$$g_{20} = 2f_{10}f_{20}$$

$$g_{21} = 2\left[f_{21}\eta_R U_1 - f_{11}f_{21} + f_{51}^2 + \sqrt{2}\ f_5 f_{51}\right]$$

$$x_J = \frac{1}{2}\left\{\frac{1}{J(J+1)} - \frac{1}{2J+1}\left[\frac{J+1}{(J-1)J} + \frac{J}{(J+1)(J+2)}\right]\right\}$$

$$g_{31} = f_{31}^2 + 2f_{31}\eta_R(U_1 - \tfrac{1}{4}) + f_{41}^2 - f_4 f_{41} + 2f_{51}^2 + \sqrt{8}\ f_5 f_{51}$$

$$g_{41} = f_{31}f_{41} + f_{41}\eta_R\left(U_1 - \frac{1}{4}\right) - \frac{1}{2}\,f_4 f_{31} + 2f_{51}^2 + \sqrt{8}\ f_{51}f_5$$

interval of incident particle energies T, by a cubic function

$$\mathrm{Re}\ \delta_\ell(T) = \sum_{i=1}^{3} \frac{a_{\ell_i}}{i!} (T - T_0)^i \ , \tag{18}$$

where T_0 is a fixed energy within this interval and where the fitted parameters $a_{\ell_0} \ldots a_{\ell_3}$ represent the value and the first three derivatives of $\delta_\ell(T)$ at $T = T_0$. The imaginary parts are parametrized by

$$\mathrm{Im}\ \delta_\ell(T) = \begin{cases} 0 & \text{for } T \le T_0 \\ \sum_{i=2}^{3} \frac{b_{\ell_i}}{i!} (T - T_{0\ell})^i & \text{for } T > T_0 \end{cases} \tag{19}$$

where the threshold energy $T_{0\ell}$ for each phase shift is treated as a free parameter, and where the coefficient b_{ℓ_2} is required to be non-negative. If the threshold is below the lower limit of the interval, the form of the energy dependence of Im δ_ℓ coincides with that of Re δ_ℓ.

For the partial waves with total angular momentum $J > J_{max}$ the contributions of OPE were included. The coupling constant f^2 can be treated as a free parameter.

The information on the inelastic processes is introduced by fitting the total cross-sections of the reactions (i) $pp \to pp\pi^0$, (ii) $pp \to pn\pi^+$ and (iii) $pp \to d\pi^+$ together with the total inelastic cross-section data [sum of (i) + (ii) + (iii)] and independent data of total cross-sections with charged pions [sum of (ii) + (iii)]. The calculated total inelastic cross-section was used instead of directly measured data.

Altogether about 2850 independent experimental data were used. These data were divided into six overlapping energy intervals: 19-150 MeV, 95-270 MeV, 170-350 MeV, 270-460 MeV, 380-610 MeV, and 560-750 MeV.

The amplitude representation used in our computation can be found in paper [13].

4. RESULTS

We have performed the phase-shift analysis in six energy regions with three different treatments of the e.m. contributions:

i) Breit formalism without taking into account the wave distortion effect (B),

ii) complete Breit formalism (BC)m

iii) our formalism (G).

to treat in a better way the forthcoming pp data at small angles from the experiments which are in progress at the meson factories at LAMPF, SIN, and TRIUMF. With the supply of these new data, an accurate treatment of the e.m. interaction will become more important, both for the pp and for the np interactions. In the future, a correct treatment of the e.m. interaction will also be important for higher energy experiments being prepared at ANL and at Saclay.

From Fig. 2 we see that the pion-nucleon $pp\pi^0$ coupling constant is determined best in the energy intervals around 140 and 260 MeV. This is strongly related to the presence of more small-angle data in these energy intervals [1]. Therefore we expect that with the new data the determination of the value of the $pp\pi^0$ coupling constant will be much more accurate. We should point out that the $pp\pi^0$ coupling constant obtained in our analysis is systematically smaller than the coupling constant obtained from πp scattering data. We expect that this question also will be resolved in the near future.

It follows from Table 3 that the inclusion of the form factors gives a significant improvement in the interpretation of the data. On the other hand, as we can see from Fig. 1, the pp data at the energies considered do not give enough information on the shape of the form factor.

Table 1

Nuclear phase shifts (in degrees) and the ratio of the real to the imaginary part of the forward-scattering spin-independent nuclear amplitude for the three cases B, BC, and G

Energy	40 MeV				90 MeV			
Re δ	B	BC	G	Max error	B	BC	G	Max error
$^1S_0$	43.20	43.20	42.91	± 0.17	28.91	28.91	28.82	± 0.42
$^3P_0$	9.91	9.80	10.32	± 0.53	9.05	9.00	9.12	± 0.70
$^3P_1$	- 6.35	- 6.42	- 6.47	± 0.21	-12.68	-12.79	-12.68	± 0.29
$^3P_2$	4.04	4.12	4.10	± 0.15	9.48	9.57	9.50	± 0.21
$^1D_2$	1.62	1.62	1.60	± 0.05	3.73	3.73	3.71	± 0.14
ε_2	- 1.78	- 1.76	- 1.58	± 0.14	- 2.27	- 2.29	- 2.17	± 0.12
$^3F_2$	- 0.71	- 0.76	- 0.88	± 0.18	- 0.42	- 0.48	- 0.68	± 0.32
$^3F_3$	0.31	0.31	0.51	± 0.26	- 0.40	- 0.42	- 0.19	± 0.28
$^3F_4$	- 0.18	- 0.16	- 0.29	± 0.10	- 0.15	- 0.09	- 0.27	± 0.19
$^1G_4$	0.06	0.06	0.10	± 0.05	0.40	0.39	0.40	± 0.08
ε_4	- 0.16	- 0.16	- 0.14	± 0.09	- 0.45	- 0.45	- 0.40	± 0.08
$^3H_4$	0.12	0.09	0.13	± 0.10	- 0.21	- 0.25	- 0.18	± 0.08
$^3H_5$	0.04	0.02	0.06	± 0.13	0.61	0.58	0.63	± 0.15
Re/Im	1.421	1.408	1.442	± 0.016	1.951	1.917	1.945	± 0.033

Table 1 (cont.)

Energy	310 MeV				430 MeV			
Re δ	B	BC	G	Max error	B	BC	G	Max error
$^1S_0$	- 6.78	- 6.63	- 7.08	± 1.25	-17.86	-17.61	-18.29	± 1.27
$^3P_0$	- 4.90	- 5.05	- 5.13	± 1.45	-16.03	-18.01	-17.58	± 1.80
$^3P_1$	-20.89	-20.78	-20.92	± 0.95	-34.07	-34.37	-34.61	± 1.09
$^3P_2$	20.72	21.08	20.84	± 0.62	18.96	18.49	18.40	± 0.69
$^1D_2$	12.05	12.07	12.07	± 0.43	13.22	13.30	13.24	± 0.55
ε_2	- 1.28	- 1.18	- 1.20	± 0.43	- 1.18	- 1.38	- 1.34	± 0.77
$^3F_2$	- 2.41	- 2.66	- 2.53	± 0.55	1.56	1.23	1.37	± 0.86
$^3F_3$	- 1.91	- 1.92	- 1.91	± 0.64	- 1.89	- 2.16	- 2.06	± 0.38
$^3F_4$	- 0.14	- 0.17	- 0.26	± 0.38	3.38	3.52	3.37	± 0.17
$^1G_4$	1.91	1.93	1.94	± 0.27	2.41	2.35	2.34	± 0.29
ε_4	- 1.07	- 1.03	- 1.05	± 0.32	- 3.20	- 3.13	- 3.19	± 0.30
$^3H_4$	- 0.43	- 0.68	- 0.56	± 0.45	0.07	0.07	0.06	± 0.38
$^3H_5$	0.04	0.08	0.12	± 0.46	- 0.54	- 0.59	- 0.51	± 0.40
$^3H_6$	- 0.21	- 0.19	- 0.24	± 0.33	0.06	0.41	0.27	± 0.29
$^1I_6$	- 0.51	- 0.49	- 0.48	± 0.21	0.45	0.42	0.43	± 0.25
ε_6	- 0.93	- 0.91	- 0.92	± 0.25	- 1.36	- 1.28	- 1.31	± 0.15
$^3J_6$	0.15	0.09	0.13	± 0.22	- 0.09	- 0.17	- 0.15	± 0.15
$^3J_7$	0.55	0.57	0.59	± 0.29	- 0.67	- 0.56	- 0.56	± 0.32
Im δ								
Im $^1S_0$	-	-	-	-	-	-	-	-
Im $^3P_1$	0.00024	0.00049	0.00166	± 0.00743	1.10	0.67	0.95	± 0.88
Im $^3P_2$	-	-	-	-	0.11	0.11	0.13	± 0.05
Im $^1D_2$	0.165	0.169	0.168	± 0.009	1.67	1.93	1.73	± 0.57
Im $^3F_2$	-	-	-	-	-	-	-	-
Im $^3F_3$	-	-	-	-	-	-	-	-
Re/Im	1.002	0.971	0.976	± 0.039	0.630	0.605	0.602	± 0.015

Table 2

Comparison of χ^2 and $\chi^2/\bar{\chi}^2$ for the three cases B, BC, and G, for different energy regions

Mean energy of interval		80 MeV	140 MeV	260 MeV	350 MeV	500 MeV	670 MeV
χ^2	B	770.39	596.14	375.81	597.50	894.07	784.02
	BC	771.15	591.91	358.17	577.13	867.80	773.13
	G	769.74	590.91	364.39	578.28	867.77	777.12
$\frac{\chi^2}{\bar{\chi}^2}$	B	1.0097	1.0087	0.9916	0.9514	1.0241	0.9644
	BC	1.0107	1.0015	0.9450	0.9190	0.9952	0.9510
	G	1.0088	0.9999	0.9615	0.9208	0.9929	0.9489

Table 3

χ^2 with and without the form factor for the case G

		Mean energy of interval (MeV)					
		80	140	260	350	500	670
Without form factor	χ^2	770.10	590.60	369.00	587.85	878.82	782.44
With form factor		769.74	590.91	364.39	578.28	867.77	777.12

Figure captions

Fig. 1 : Dependence of χ^2 on the dipole mass m_D for the case G.

Fig. 2 : Dependence of χ^2 on the coupling constant f^2 for the case G. An arbitrary constant is subtracted from each curve.

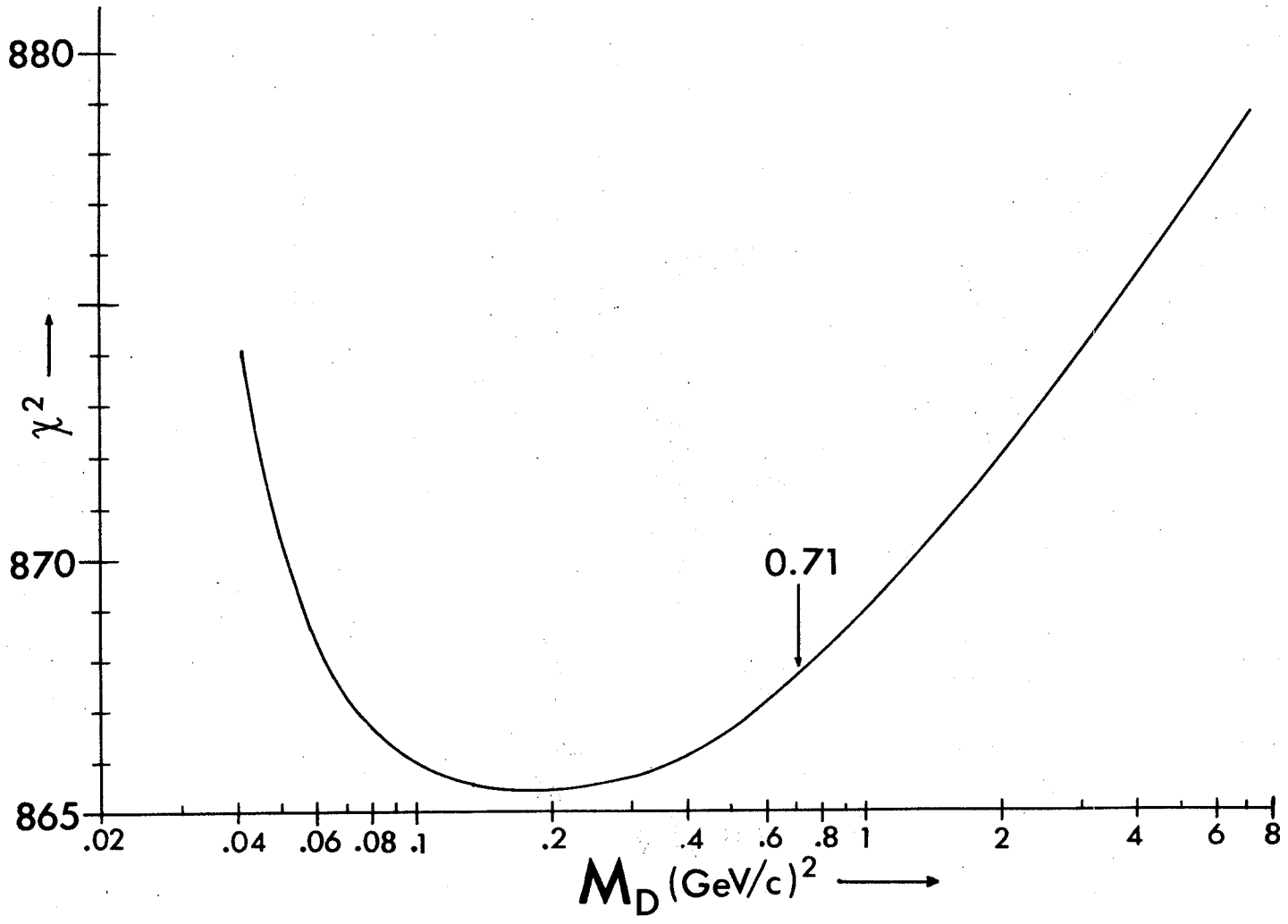

Fig. 1